

# A Non-Linear Beam Dynamics Experiments at VEPP-4M Ring

V.Kiselev, E.Levichev, I.Protopopov, V.Sajaev, V.Smaluk,  
Budker Institute of Nuclear Physics, 630090 Novosibirsk, Russia

## Abstract

Nonlinear dynamics of transverse beam motion have been studied experimentally at the VEPP-4M electron-positron collider. The following aspects of non-linear beam behavior were investigated: the dynamic aperture reduction due to the chromatic sextupoles, the amplitude dependent tune shift and phase space topology near the nonlinear resonances. The results of the observations are presented and compared with the theoretical estimations.

## 1 INTRODUCTION

This paper describes the results of the nonlinear dynamics experiments which were performed at VEPP-4M storage ring in 1995-1996. The main goals of these experiments were: studying of the essential aspects of the single particle dynamics (phase space distortion, amplitude dependent tune shift and dynamic aperture limitation); finding the ways to control the nonlinear effects and increase the dynamic aperture, and checking the validity of the theoretical predictions.

## 2 HARDWARE DESCRIPTION

The VEPP-4M storage ring is a 6 GeV racetrack electron-positron collider with a circumference of 366 m. This study was performed at the injection energy of 1.8 GeV. The relevant parameters of VEPP-4M at this energy are given in Table:

Energy	1.8 GeV
Revolution period	1.2 $\mu$ s
Betatron tunes (h/v)	8.620/7.560
Natural chromaticity (h/v)	-13.6/-20.7
Horizontal emittance	35 nm-rad
Rms beam bunch length	6 cm
Damping times (h/v/long.)	35 ms/70 ms/70 ms

To produce the coherent transverse motion, the beam is kicked vertically or horizontally with the pulsed electromagnetic kicker. The pulse duration is 50 ns for the horizontal kicker and 150 ns for the vertical one. The oscillation of the beam centroid and beam intensity are measured turn-by-turn with beam position monitor, BPM, for 1024 revolutions. The measured BPM rms resolution in 1 to 5 mA beam current range is  $\sigma_{x,z} \simeq 70 \mu$ m.

## 3 PHASE SPACE TRAJECTORIES

We have been tracking the motion of the beam centroid using single BPM only [3]. To illustrate our approach let us

consider the horizontal betatron oscillation at the BPM azimuth

$$x(n) = a\beta_x^{1/2} \cos 2\pi n\nu_x,$$

$$x'(n) = -a/\beta_x^{1/2} [\alpha_x \cos 2\pi n\nu_x + \sin 2\pi n\nu_x], \quad (1)$$

where  $\alpha_x = -1/2\beta'_x(s)$  and  $\beta_x(s)$  are the betatron functions and phase advance for  $n$ th turn is equal to  $2\pi n\nu_x$ . This expression can be rewritten in the form

$$x'(n) = [x_{\pi/2}(n) - \alpha_x x(n)]/\beta_x, \quad (2)$$

where  $x_{\pi/2}(n)$  is the coordinate that would be measured by the "pseudo"-BPM placed at the azimuth which corresponds to the following conditions: (i)  $\alpha_x$ ,  $\beta_x$  here are the same as for the first BPM, (ii) the betatron phase shift between two BPMs is exactly  $\pi/2$ , and (iii) the beam path from the first BPM to the second one is free from nonlinearities. We refer to this second BPM as "pseudo"-BPM because it is impossible in practice to meet all the requirements mentioned above. Introducing the "angle-action" variables ( $J_x$ ,  $\phi_x$ ) as usual [2] and substituting (1) we can obtain

$$J_x(n) = (x_{\pi/2}^2(n) + x^2(n))/2\beta_x, \quad (3)$$

$$\tan \phi_x(n) = x_{\pi/2}(n)/x(n).$$

One can see that  $\alpha_x$  is canceled from the expression for  $J_x(\phi_x)$  and phase curves demonstrate a "mere" nonlinear distortion.

Applying FFT to the array of  $x(n)$  measured by BPM and using few main harmonics to construct the coordinates  $X(n)$ , the rules for harmonics transformation can be found to obtain the array of  $X'(n)$ . This approach was verified with computer tracking and compared also with usual approach on VEPP-4M when two BPMs were used with  $\pi/2$  betatron phase shift between them. Fig.1 shows the usual two BMPs technique.

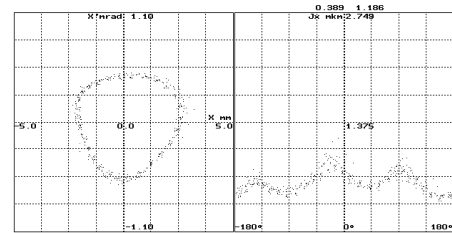


Figure 1: Phase space measured with usual two BPMs technique.

Fig.2 demonstrates the agreement between the measured horizontal phase trajectory and that simulated by tracking

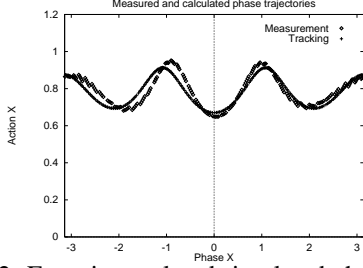


Figure 2: Experimental and simulated phase trajectories.

code. The correspondence seems quite impressive. Fig.3 shows the phase space topology near the resonance  $4\nu_x = 35$  and directly at this resonance (two BPMs without harmonic decomposition).

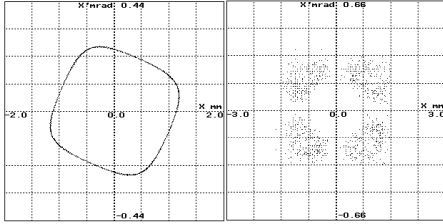


Figure 3: Phase trajectories near and at resonance  $4\nu_x = 35$ . The latter plot does not use harmonic decomposition.

High spectral resolution permits to estimate the parameters of the nonlinear system. We have extracted the amplitude of the  $3\nu_x = 26$  resonance driving term from the measured data and compared it with that calculated from the nonlinear Hamiltonian [4]. The agreement seems not bad: the experimental value is of  $A_{3\ 26} = -2.9 \pm 1.0 \text{ m}^{-1/2}$  while the theoretical one is of  $A_{3\ 26} = -2.1 \text{ m}^{-1/2}$ .

## 4 AMPLITUDE DEPENDENT TUNE SHIFT

Nonlinear detuning was studied with the same turn-by-turn technique. The coherent beam oscillations were fired by several kicker pulses with different amplitudes, and tune was extracted from the FFT spectrum. The accuracy of the tune measurement is better than  $\delta\nu = 2 \cdot 10^{-4}$ .

A nonlinear tune shift is proportional to the square of the initial beam displacement independently of octupole or sextupole field causes it. A general 2D form of the amplitude dependent tune shifts can be expressed as (second order approximation):

$$\begin{aligned}\Delta\nu_x(a_x, a_z) &= C_{11}a_x^2 + C_{12}a_z^2, \\ \Delta\nu_z(a_x, a_z) &= C_{21}a_x^2 + C_{22}a_z^2,\end{aligned}\quad (4)$$

where  $C_{nm}$  depends on particular perturbative potential. The measured and estimated coefficients values are listed in Table

$C_{nm} \cdot 10^4$	Theory	Experiment
$C_{11}$	0.1	9.0
$C_{12}$	-0.6	-1.0
$C_{21}$	-1.9	-4.0
$C_{22}$	-0.6	-1.0

The difference in theoretical and experimental  $C_{11}$  has motivated us to explore systematically the horizontal non-linearity of the ring. We have used the difference between octupole and sextupole induced tune shift to distinguish which one defines  $C_{11}$  in our case. For the octupole potential, horizontal tune shift is independent of initial tune value and is written as [5]

$$\Delta\nu_x^{(o)}(J_x) = \frac{J_x}{16\pi} \int_0^C \mathcal{O}(s) \beta_x^2(s) ds + o(J_x^2), \quad (5)$$

where  $C$  is the machine circumference and  $\mathcal{O}(s) = (d^3 B_z(s)/dx^3)/B\rho$  is the effective octupole strength. On the contrary, sextupole induced tune shift depends on the initial tune in a resonant way and near the resonance  $3\nu_{x0} \simeq m$  can be written as

$$\Delta\nu_x^{(s)}(J_x) \simeq -J_x \cdot 36 \frac{A_{3m}^2}{3\nu_x - m} + o(J_x^2), \quad (6)$$

$$A_{3m} = \frac{1}{48\pi} \int_0^{2\pi} \beta_x^{3/2} \mathcal{S} \cos(3(\psi_x - \nu_x \theta) + m\theta) d\theta,$$

where  $\mathcal{S}(s) = (d^2 B_z(s)/dx^2)/B\rho$  is the effective sextupole strength and  $A_{3m}$  is the azimuthal harmonic of the sextupole perturbation Hamiltonian.

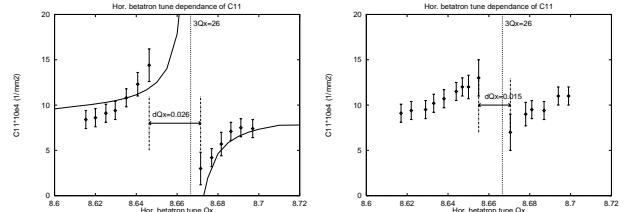


Figure 4: Left: nonlinear detuning near the resonance  $3\nu_x = 26$ . Solid line - theoretical prediction. Resonance width  $\Delta\nu_x = 0.026$ . Right: same as left but with the resonance driving term reduced. Note that the resonance width is decreased in a factor of 2.

The measurement of the horizontal tune shift as a function of the initial tune value  $\nu_{x0}$  around the resonance  $3\nu_{x0} = 26$  shows (Fig.4, left) that the resulting nonlinear detuning in the working point is induced both by sextupole and octupole perturbations. First one demonstrates typical resonant behavior, while second one produces constant "background" with the value of  $\Delta\nu_x^{(o)}/a_x^2 \simeq 8 \cdot 10^{-4} \text{ mm}^{-2}$ . The octupole correctors can control the "background" value while the resonant behavior of the sextupole detuning component remains the same. And vice versa, when we have decreased the strength of the strong sextupole lenses in interaction region and compensated the chromaticity with the sextupole correctors distributed around the ring, we saw that it does not influence on the octupole "background" but significantly reduces the sextupole component (together with the resonance width), as it seen in Fig.4 (right).

The source of rather high octupole nonlinearity has not yet understood and more vigorous study is required. As a probable candidate we consider nonlinear errors in the Final Focus quadrupoles.

## 5 DYNAMIC APERTURE

Dynamic aperture studies are being carried out also on VEPP-4M with the same turn-by-turn diagnostic technique

but now besides the beam displacement, the beam loss measurement is required to define the dynamic or physical aperture limit.

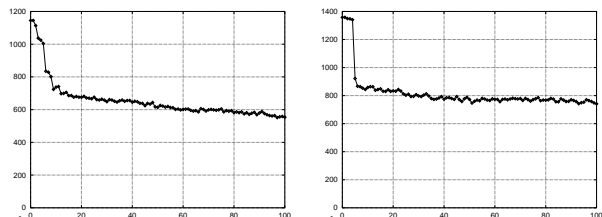


Figure 5: Fast beam loss at dynamic (left) and physical (right) apertures. Plot presents first 100 turns.

To be assure that the particles loss is really connected with the boundary of the stable area, we have explored the process of particles escaping from the tail of beam distribution. We have found that to determine the aperture limit with turn-by-turn loss measurements it is important to consider first 20-40 revolutions of the beam (Fig.5, left). A long observation includes many other effects and cannot be a figure of merit for the aperture measurement. For instance, the beam intensity decreasing measured with a current transformer depends on the initial beam current that points to the probable coherent instabilities which take part in the beam loss. Fast intensity loss allows us to distinguish between dynamic and physical aperture limitation. The first one displays the intensity reducing during few tens turns because the oscillation amplitude grows at resonance fast but not immediately while the second one occurs for the very few revolutions (it depends on the fractional tune value). Fig.5 (right) shows the beam loss at the knife of the movable scraper.

Another one difference between computer and experimental tracking near the border of stable area is a finite beam size: when the tail of the transverse beam distribution is cut off by the aperture limit, the BPM readings became wrong. We have calculated this effect assuming a Gaussian beam density distribution and results agree rather good to those obtained from experiment.

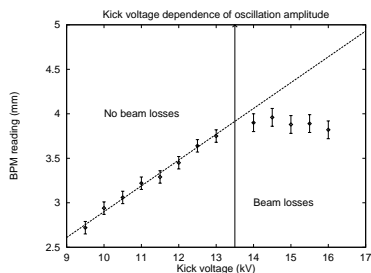


Figure 6: BPM reading versus kick voltage.

To correct the BPM position measurements we used linear correspondence between kick voltage and beam position (see fig.6). The coefficient was measured at low amplitude before performing aperture measurements. We determined the aperture boundary as the displacement at which beam lost the half of its initial intensity. With this methodic, the following aperture limits were measured at the azimuth of

BPM *SRP3*:

$$A_x = 4.5\text{ mm}, (\beta_x = 4\text{ m}); \quad A_z = 5.1\text{ mm}, (\beta_z = 22\text{ m}).$$

The beam loss profile for the first few tens turns shows that for the horizontal direction, the aperture is defined by the nonlinear processes while vertical aperture is determined by the physical limitation.

To check the value of the horizontal dynamic aperture, the tracking simulation and the analytical calculation by perturbative approach were performed. Both of them predict similar value for the stable motion boundary ( $A_x \simeq 4.3$  mm) which nicely corresponds to those obtained from experiment.

To increase the dynamic aperture we have tried the following cures: (a) decreasing of the main sextupole driving term as we described above; (b) reducing of  $C_{11}$  value by the octupole corrections; (c) combination of both (a) and (b) techniques. The case (a) demonstrates rather good result: the horizontal dynamic aperture is increased up to  $A_x = 7$  mm while in cases (b) and (c) the increasing is almost the same and small ( $A_x = 5 - 5.8$  mm).

## 6 REFERENCES

- [1] P.L.Morton et al."A diagnostic for dynamic aperture", SLAC-PUB-3627. J.Bridges et al."Dynamic aperture measurement on Aladdin", PA, 1990, Vol.28, pp.1-9.
- [2] A. Ando."Distortion of beam emittance with nonlinear magnetic fields", PA 15 (1984), p.177.
- [3] A.Kalinin at al. Applications of beam diagnostic system at the VEPP-4 complex. These proceedings.
- [4] E. Levichev and V. Sajaev."Nonlinear Dynamics Study of the SIBERIA-2 Electron Storage Ring", AIP Proc.344, p.160-169, 1995.
- [5] R.A. Bech, R. Belbeoch and G. Gendreau. Shifts in Betatron Frequencies Due to Energy Spread, Betatron Amplitudes and Closed Orbit Excursions.- Proc. of the Conf. HEAC, Cambridge (1967), A-63.